第 44 卷第 8 期
2015 年 8 月

光 子 学 报
ACTA PHOTONICA SINICA

Vol. 44 No. 8
August 2015

量子光力系统中激光额外噪声的高效抑制

张新艳,李宗阳,李永民

（山西大学 光电研究所 量子光学与光量子器件国家重点实验室,太原 030006）

摘　要：采用级联非平衡马赫-曾德光纤干涉仪来降低激光额外噪声,并实验证明了其可行性及激光噪声抑制效果. 当光纤干涉仪两臂长度差为 127 m 时,通过自制的自动相位锁定装置,可以长时间稳定地将干涉仪两臂的相对相位锁定在零相位,此时激光光场在 800 kHz 及其整数倍频率处的额外噪声得到高效地抑制,降低幅度可达 45 dB 以上. 调节干涉仪的两臂差,可以改变噪声过滤的频段. 基于该方法的噪声抑制装置结构紧凑、成本低,可应用于量子光力系统中散粒噪声极限光场的获得.

关键词：激光噪声抑制;级联非平衡马赫-曾德光纤干涉仪;相位锁定;量子光力

中图分类号：O431.2；O439　　　**文献标识码**：A　　　**文章编号**：1004-4213(2015)08-0827001-6

Efficient Suppression of Laser Excess Noises for Quantum Optomechanical System

ZHANG Xin-yan，LI Zong-yang，LI Yong-min

（*State Key Laboratory of Quantum Optics and Quantum Optics Devices*，*Institute of Opto-Electronics*，*Shanxi University*，*Taiyuan* 030006，*China*）

Abstract：The suppression of laser excess noise using a cascaded imbalanced Mach-Zehnder interferometer with fiber optic components was proposed and demonstrated in the experiment. By developing an automatic phase control system，the phase of the fiber interferometer with a large path imbalance (127 m) can be stabilized in a long term，and the laser excess noise around 800 kHz and its integer multiples can be efficiently suppressed by more than 45 dB. The effective frequency bands of the noise filter can be controlled by adjusting the arm-length difference of the interferometer. The approach provides an effective solution for achieving compact and cost-effective laser noise reduction，and can be applied directly to the quantum optomechanical system where shot-noise-limited laser can be required.

Key words：Laser noise suppression；Cascaded imbalanced fiber Mach-Zehnder interferometer；Phase locking；Quantum optomechanics

OCIS Codes：270.0270；350.2460；060.2310

0　Introduction

For various high precision optical measurement fields，such as gravitational wave detection[1-3] and laser ultrasonic inspection[4]，high resolution optical interferometers are usually employed. In these applications，a high-performance single frequency laser is required. The solid-state lasers are traditional optical sources which can provide a high power coherent emission with narrow linewidth and good stability. Recently the maturity of single frequency semiconductor lasers and fiber lasers are becoming alternatives for such optical measurements. However，all of these above laser sources suffer from large excess noises far above the shot noise level. Such excess frequency and intensity noises of the laser can degrade the measurement sensitivity. To achieve the shot noise limit performance，the fluctuations of the laser sources

should be suppressed to reach the shot-noise level. Furthermore, low noise (shot-noise-limited) lasers are also crucial to the performance of the atom interferometry[5], preparation of nonclassical states of light[6-7], entangled states of atoms[8], and most recent quantum optomechanics[9-13].

In order to reduce the laser excess noises, several approaches have been proposed and demonstrated. An active feedback loop has been demonstrated to suppress the relaxation oscillation of a Nd:YAG laser[14-15]. It is noted that this method is only effective for the intensity noise. Narrow linewidth Fabry-Perot cavity[16-17] can well reduce both the frequency and intensity noises at the frequency range above the linewidth of the cavity. This method usually demands the high finesse cavity and a sophisticated servo system, which will result in a complex and costly system. For instance, in order to reduce the laser noise at a low frequency band less than 1 MHz, a very high finesse cavity with linewidth of 8.6 kHz was employed[17], furthermore, a vacuum chamber was also involved to isolate the environment noises and prevent contamination of the cavity mirrors. Compared with the high-finesse Fabry-Perot cavity where the light field propagates in free space, a passive fiber ring cavity[18-19] can easily attain very narrow linewidth due to the long lengths of intra-cavity fiber. However, the output power from such device is limited by the Stimulated Brillouin Scattering (SBS) threshold which has a typical value of several hundreds of microwatts.

In this paper, we propose an approach for efficient reduction of laser excess noise using a cascaded Imbalanced Mach-Zehnder Interferometer (IMZI)[20-22] with fiber optic components and demonstrate. To this end, an automatic phase control system is developed and the fiber interferometer with a 127 m path imbalance could stay locked stably in a long term. The laser excess noise is significantly reduced by more than 45 dB at targeted frequency bands where low laser noises are required. Because no fiber cavity is involved, our approach is robust to the SBS and can handle higher laser power with the order of several tens of milliwatt. The presented system eliminates the requirements of high finesse cavity and vacuum system, and allows for efficient laser noise reduction at frequency band below one megahertz with only compact and cost-effective fiber devices.

This approach can be used for the suppression of laser excess noises at the frequency band of phonon modes in optomechanical experiments based on Si3N4 membranes[9-11] where the typical frequencies of the low order phonon modes are around 1 MHz. Such these excess noises can preclude ground-state cooling of optomechanical systems[12-13].

1 Theoretical analysis

The basic unit of our noise eater is an IMZI with an arm-length difference of ΔL, as shown in Fig. 1(a). The input mode $\hat{A}_{in}$ mixes with the vacuum field $\hat{A}_{v1}$ at a 50 : 50 Beam-Splitter (BS) and two output modes $\hat{A}_r$ and $\hat{A}_t$ are obtained. The two emerging modes then travel via different paths which introduce a delay time τ and recombine at a second 50 : 50 BS. Finally two output modes $\hat{A}_{out1}$ and $\hat{A}_{out2}$ are produced. Noted that ΔL is much larger than the optical wavelength and can introduce a frequency-dependent phase shift. If the relative optical phase shift of the carrier (ω_0) of the input mode is set to be $\phi = 2m\pi$ (m is an integer) and the delay time is set to be $\omega\tau = (2n+1)\pi$ (n is an integer and ω is the RF frequency of the side mode), the carrier mode and the RF sideband mode will undergo different phase shift and radiate from different output ports of the IMZI due to the constructive interference and destructive interference, respectively. Therefore, the laser excess noise at certain frequencies of ω can be eliminated.

(a) Cascaded imbalanced Mach-Zehnder interferometer

EOM: electro-optical amplitude modulator; BS, BS$_1$-BS$_3$: 50:50 beam splitters; PZT: piezoelectric transducer; API: automatic proportional-integral controller

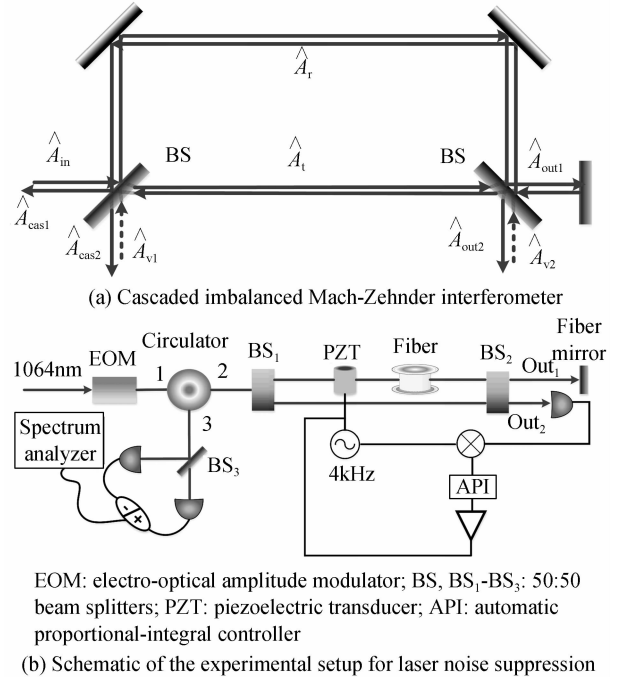(b) Schematic of the experimental setup for laser noise suppression

Fig. 1　Schematic of the cascaded imbalanced Mach-Zehnder interferometer and the experimental setup

We assume that the single frequency input laser is relatively intense and the input fields are given by

$$\hat{A}_{in}(t) = \alpha + \delta\hat{A}_{in}(t) \qquad (1)$$

$$\hat{A}_{v1}(t) = \delta\hat{A}_{v1}(t) \qquad (2)$$

where $\hat{A}_{in}(t)$ is the input field, α is its classical mean amplitude (α is assumed to be real), $\delta\hat{A}_{in}(t)$ represent

the time-varying component of the field including both the classical and quantum fluctuations of the input field, $\hat{A}_{v1}(t)$ and $\delta \hat{A}_{v1}(t)$ represent the vacuum field. The two emerging modes just before the second BS can be written as

$$\hat{A}_r(t)=\frac{1}{\sqrt{2}}e^{i\phi}[-\hat{A}_{in}(t-\tau)+\hat{A}_{v1}(t-\tau)] \tag{3}$$

$$\hat{A}_t(t)=\frac{1}{\sqrt{2}}[\hat{A}_{in}(t)+\hat{A}_{v1}(t)] \tag{4}$$

where $\tau=\Delta L/c$ and $\varphi=\omega_0\tau$ are the delay time and phase shift introduced by the arm-length difference ΔL (ΔL is the optical path length) of the IMZI, ω_0 is the carrier frequency. Finally, the output fields from the single-pass IMZI can be given by

$$\hat{A}_{out1}(t)=\frac{1}{\sqrt{2}}(\hat{A}_t(t)-\hat{A}_r(t))=\frac{1}{2}\alpha(1+e^{i\phi})+$$
$$\frac{1}{2}[\delta\hat{A}_{in}(t)+\delta\hat{A}_{v1}(t)+e^{i\phi}(\delta\hat{A}_{in}(t-\tau)-$$
$$\delta\hat{A}_{v1}(t-\tau))] \tag{5}$$

$$\hat{A}_{out2}(t)=\frac{1}{\sqrt{2}}(\hat{A}_r(t)+\hat{A}_t(t)) \tag{6}$$

The field quadrature operator is defined as $\hat{X}^\theta(t)=e^{-i\theta}\hat{A}(t)+e^{i\theta}\hat{A}^\dagger(t)$, and the corresponding fluctuation in the quadrature is then given by

$$\delta\hat{X}^\theta_{out1}(t)=\frac{1}{2}[\delta\hat{X}^\theta_{in}(t)+\delta\hat{X}^\theta_{v1}(t)+$$
$$e^{i\varphi}(\delta\hat{X}^\theta_{in}(t-\tau)-\delta\hat{X}^\theta_{v1}(t-\tau))] \tag{7}$$

By means of a Fourier transform, Eq. (7) can be rewritten as

$$\delta\hat{X}^\theta_{out1}(\omega)=\frac{1}{2}[\delta\hat{X}^\theta_{in}(\omega)+\delta\hat{X}^\theta_{v1}(\omega)+$$
$$e^{i\phi}e^{-i\omega\tau}(\delta\hat{X}^\theta_{in}(\omega)-\delta\hat{X}^\theta_{v1}(\omega))] \tag{8}$$

Adjusting the optical phase of the carrier frequency to $\phi=2m\pi$ (m is an integer), the noise spectrum for the output field $\hat{A}_{out1}$ is

$$\langle|\delta\hat{X}^\theta_{out1}(\omega)|^2\rangle=\cos^2(\omega\tau/2)\langle|\delta\hat{X}^\theta_{in}(\omega)|^2\rangle+$$
$$\sin^2(\omega\tau/2)\langle|\delta\hat{X}^\theta_{v1}(\omega)|^2\rangle \tag{9}$$

By using the similar procedure, the noise spectrum for the output field $\hat{A}_{out2}$ can also be obtained

$$\langle|\delta\hat{X}^\theta_{out2}(\omega)|^2\rangle=\cos^2(\omega\tau/2)\langle|\delta\hat{X}^\theta_{v1}(\omega)|^2\rangle+$$
$$\sin^2(\omega\tau/2)\langle|\delta\hat{X}^\theta_{in}(\omega)|^2\rangle \tag{10}$$

For $\phi=2m\pi$, due to constructive interference of the carrier of the input optical field, one have $\langle\hat{A}_{out1}(t)\rangle=\alpha$ from Eq. (5). If the delay time τ is further adjusted to $\tau=\pi/\Omega_0$, here Ω_0 is the targeted sideband frequency at which the excess noise will be removed, Eq. (9) can be rewritten as

$$\langle|\delta\hat{X}^\theta_{out1}(\omega)|^2\rangle=\cos^2[\omega\pi/(2\omega_0)]\langle|\delta\hat{X}^\theta_{in}(\omega)|^2\rangle+$$
$$\sin^2[\omega\pi/(2\omega_0)]\langle|\delta\hat{X}^\theta_{v1}(\omega)|^2\rangle \tag{11}$$

Therefore, the excess noises at the sideband frequencies $(2n+1)\Omega_0$ (n is an integer) can be eliminated completely and the output laser field $\hat{A}_{out1}$ can reach the shot noise limit due to the destructive interference of the sideband modes. It is noted that this noise filtering only works within discrete narrow frequency bands around the center frequency $(2n+1)\Omega_0$. To extend the effective frequency bands of the noise filter, a cascaded noise filtering scheme can be utilized in which the transmitted light is reinjected into the IMZI for a second passage to improve the filtering effect. In this case, the noise spectrum of output field $\hat{A}_{cas1}$ by a double-pass through the IMZI is given by

$$\langle|\delta\hat{X}^\theta_{cas1}(\omega)|^2\rangle=\cos^4[\omega\pi/(2\Omega_0)]\langle|\delta\hat{X}^\theta_{in}(\omega)|^2\rangle+$$
$$\sin^2[\omega\pi/(2\Omega_0)]\{\langle|\delta\hat{X}^\theta_{v2}(\omega)|^2\rangle+$$
$$\cos^2[\omega\pi/(2\Omega_0)]\langle|\delta\hat{X}^\theta_{v1}(\omega)|^2\rangle\} \tag{12}$$

Given the targeted frequency of $\Omega_0=2\pi\times810$ kHz, Fig. 2 (a) and (b) shows the theoretical simulations of the single-pass and double-pass noise suppression, respectively. In Fig. 2 we assume that the noise power of input field is 50 dB above the shot-noise level $\langle|\delta\hat{X}^\theta_{in}(\omega)|^2\rangle=10^5$ (shot noise unit). It is evident that the double-pass configuration effectively extends the bandwidth of noise filtering. In Fig. 3, the
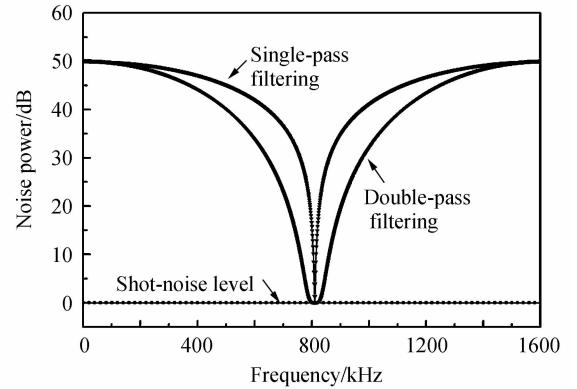

Fig. 2 Simulations of the noise filtering at the targeted frequency of 810 kHz
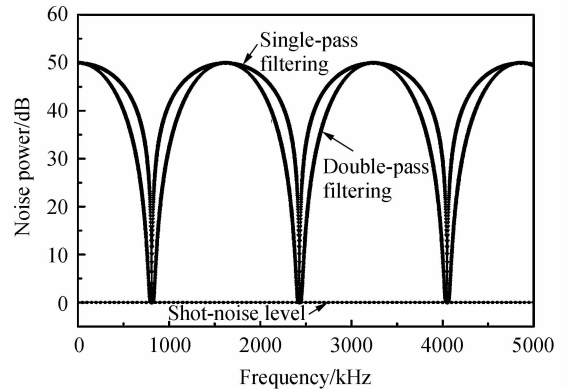

Fig. 3 Periodic laser noise suppression where the notch frequencies satisfy $\omega=(2n+1)\Omega_0$, and $\Omega_0=2\pi\times810$ kHz

reduction of the laser excess noise is shown at an extended frequency range. A periodic laser noise suppression can be observed where the notch frequencies satisfy $\omega = (2n+1)\Omega_0$, here n is an integer.

2 Experimental results and discussions

The schematic of the experimental setup is shown in Fig. 1(b). The light source is a single frequency continuous wave Nd:YAG laser at 1 064 nm. To verify the performance of our noise filter, a high excess-noise laser field is required. Since our laser exhibits relatively low noise, an electro-optical amplitude modulator driven by white noises was utilized to modulate the amplitude of laser. As a result, an output light field with excess intensity noise approximately 50 dB above the shot-noise level is prepared.

The modulated laser is coupled to a fiber circulator and then entered the IMZI which consists of polarization-maintaining fiber components. Two 50 : 50 fiber beam splitters and a length of fiber with 127 m long form the IMZI. The arm-length difference of 127 m is determined by the targeted frequency $\Omega_0 = 810$ kHz and $\Delta L_{fiber} = \pi c/(n\Omega_0)$, here $c = 3 \times 10^8$ m/s is the speed of light in vacuum, $n = 1.445$ is the refractive index of fiber core at 1064 nm. To enable the optical phase adjusting, a fiber stretcher is constructed by winding part of the fiber onto a cylindrical Piezoelectric Transducer (PZT). By changing the applied voltage of the PZT, the fiber will be stretched and hence a fiber phase shifter is realized. The optical phase can be shifted about 40π when the voltage applied to the PZT reaches 100 volts. By adjusting the relative phase of the IMZI to be zero, constructive interference will take place at out1 of the IMZI, while the out2 where destructive interface occurs provided the light for phase locking loop. To make a double-pass configuration, a fiber mirror is connected to the out1 port, which reflects the filtered light field by single-pass back to the IMZI. The resulting light field filtered by double-pass finally comes out of the filter setup from port 3 of the fiber circulator.

A dither-locking method with a modulation frequency of 4 kHz is used to lock the relative phase of the IMZI to zero degree. The light radiated from out2 of the IMZI is received by a high sensitive photodetector and the detected RF signal is mixed down with a properly phase-shifted local oscillator to produce an error signal. The error signal is sent to an Automatic Proportional-Integral controller (API) and the output signal is amplified and feed back to the PZT to achieve the phase locking. It should be noted that once the single-pass IMZI is phase locked, the cascaded IMZI is locked correspondingly due to the same optical paths shared by the forward and backward IMZI. To isolate the mechanical vibrations which are harmful to the phase locking loop, the fiber IMZI is placed inside an anechoic chamber. By using above techniques, the IMZI could stay locked for one minute or so.

The long-term stable phase-locking is necessary for the normal operation of the system. It is found that the main limitation for the locking is due to the temperature fluctuations of the environment, which is crucial to the phase locking of the IMZI with a large path imbalance (127 m here). For fused silica single mode fibers used here, the typical thermo-optic coefficient is $9.2 \times 10^{-6}/℃$ and thermal expansion coefficient is $5.5 \times 10^{-7}/℃$. The corresponding phase shift per degree centigrade for 127 m fiber can be calculated to be $1102 \times 2\pi/℃$, which is much larger than the maximum feedback phase shift (40π) that can be provided by our fiber stretcher. To decrease the effect of temperature variations, we install the 127 m fiber into a temperature-controlled oven with stability of 0.01℃. In this case, the IMZI could stay locked for more than one hour until the output of the servo system reaches its maximum value.

In our experiment, the fiber is wound on a spool made of plastic and then enclosed in the oven. This results in low thermal conductivity and degrades temperature stability of the fiber. Further extending of the locking time can be achieved by improving the thermal contact between the oven and the fiber to ensure a low thermal contact resistance. Meanwhile, one can increase the fiber length wound onto the PZT to extend the range of feedback phase shift. A combination of above two methods will improve significantly the duration of the phase locking.

In our current system, to facilitate the locking when the system loses lock, we design an automatic servo system which can relock the IMZI automatically within 20 milliseconds once the system loses lock. The basic building block of the automatic servo system is the API (Fig. 4). The API consists of five parts, an integrator, an operational amplifier, an absolute value circuit, a comparator, and a photovoltaic relay. Whenever the output voltage of the API exceeds ± 10 V, the voltage comparator will output a high level signal. This signal can trigger the photovoltaic relay to switch-off, which provides a discharge path for the integrator capacitor C_1 and resets the integrator. The discharge process continues until the output voltage of the API returns to less than ± 0.5 V, at this stage, the voltage comparator will output a low level signal which will cause the photovoltaic relay to switch-on. Then the integrator capacitor C_1 will begin to charge again and the locking process restarts. Above

procedure will be repeated whenever the output voltage of the API exceeds ± 10 V and enabled an automatic phase locking of the IMZI.
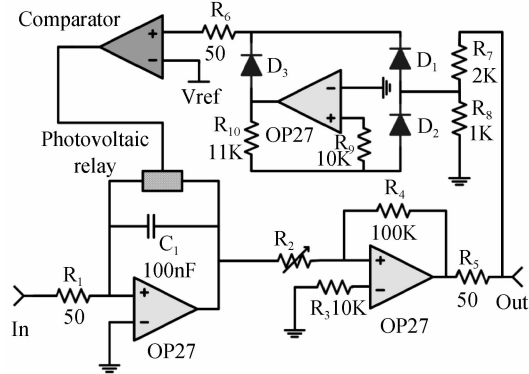

Fig. 4　Automatic proportional-integral controller

To measure the intensity noise of the laser, a self-homodyne detector which is built from two ETX-500 (JDSU) photodiodes are employed and the detected photocurrent signals are analyzed by a spectrum analyzer. The noise power of the difference photocurrent signal and the sum photocurrent signal correspond to the shot noise level and the intensity noise, respectively. Fig. 5 shows the measured laser noise spectra from 400 kHz to 1.2 MHz with a detected light power of 410 μw (the settings of the spectrum analyzer: resolution bandwidth is 2 kHz and video bandwidth is 51 Hz). Trace e represents the electronic dark noise and trace d is the shot-noise level. Trace a denotes the intensity noise of the input laser which is more than 50 dB above the shot-noise level. Trace b and c plots noise spectrum of the filtered laser for single-pass filtering and double-pass filtering, respectively. For single-pass filtering, around 40 dB of noise suppression can be observed at 800 kHz. The noise filtering effect is significantly enhanced by the double-pass scheme, the dip of the noise suppression is deeper and much wider and about 48 dB of noise reduction is achieved. Fig. 6 plots the noise filtering results from 400 kHz to 8 MHz (the settings of the
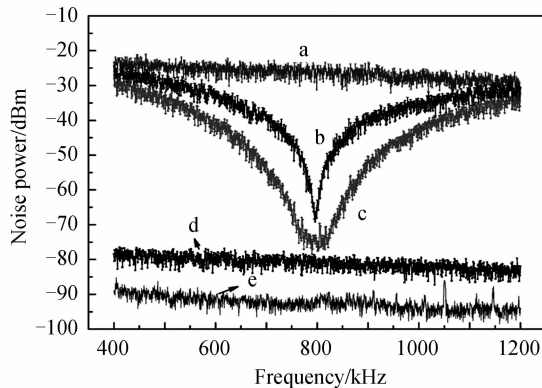

Fig. 5　The noise spectra of the filtered laser from 400 kHz to 1.2 MHz
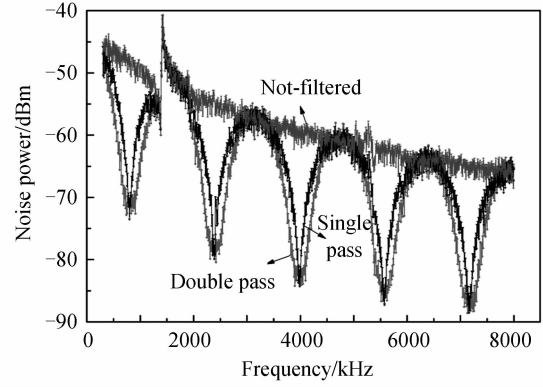

Fig. 6　The noise spectra of the filtered laser from 400 kHz to 8 MHz. Periodic laser noise suppression can be observed

spectrum analyzer: resolution bandwidth is 15 kHz and video bandwidth is 200 Hz). As expected, a periodic noise suppression is observed clearly, which is in consistent with the theoretical prediction (the noise peak around 1.4 MHz is due to the modulation error).

In principle, one can obtain a perfect noise reduction, i. e. , infinite noise filtering at the targeted frequency $\omega = (2n+1)\Omega_0$. However, the realistic noise suppression is inevitably limited by the non-ideal fiber devices. For instance, the imbalanced splitting of 50 : 50 fiber beam-splitter and unequal losses introduced by the two arms of the IMZI, both can lead to incomplete interference. The finite return loss of the fiber components in our system is another possible issue, i. e. , a small portion of the noisy input laser is reflected back directly and directed to the port3 of the fiber circulator without been filtered.

In our experiment, the total transmission ratio of the IMZI is ~21%. The loss is mainly coming from the fiber circulator (~3 dB for Ports 1-2 plus 2-3), fiber 50 : 50 beam splitter (~1 dB for each piece, single pass including connectors). By using better low-loss fiber components and employing the technique of fusion splicing rather than fiber connectors currently utilized in our system, one can reduce the inserting loss significantly and transmission ratio higher than 50% can be expected. For high power operation, one should be careful to the influence of the SBS. According to the experimental results of Ref. [18], the estimated SBS threshold of our system is around 100 mW. Experimentally, we inject up to 50 mW of laser into the IMZI and no SBS phenomenon is observed. Another issue is the spontaneous Brillouin scattering, i. e. Guided Acoustic Wave Brillouin Scattering (GAWBS) in the fiber, which can introduce excess noise to the laser even if the input power is below the SBS threshold. However, it is known that the scattering spectrum of GAWBS is discrete and the

frequency of the lowest mode is beyond 20 MHz [23]. For such a low frequency range considered here, the influence of these noises are trivial.

3 Conclusion

We have proposed and experimentally implemented an efficient filtering system for laser excess noise based on a cascaded imbalanced Mach-Zehnder interferometer. By properly adjusting the arm-length difference of the interferometer, the excess noises of the laser field at specific frequency bands can be suppressed greatly. The presented device utilizes the fiber components and has the merits of simple, compact, and low-cost. This system will be used in our optomechanical experiments based on Si3N4 membranes whose frequency of fundamental mode is around 800 kHz. Besides above application, this system may find potential applications in the fields of precision optical measurements, quantum optics, etc.

References

[1] KWEE P, BOGAN C, DANZMANN K, et al. Stabilized high-power laser system for the gravitational wave detector advanced LIGO[J]. Optics Express, 2012, 20(10): 10617-10634.

[2] WINKLER W, DANZMANN K, GROTE H, et al. The GEO 600 core optics[J]. Optics Communications, 2007, 280(2): 492-499.

[3] NAGANO S, BARTON M A, ISHIZUKA H. Development of a light source with an injection-locked Nd:YAG laser and a ring-mode cleaner for the TAMA 300 gravitational-wave detector[J]. Review of Scientific Instruments, 2002, 73(5): 2136-2142.

[4] DUBOIS M, BURR K C, DRAKE T E. Laser phase noise reduction for industrial interferometric applications [J]. Applied Optics, 2004, 43(22): 4399-4407.

[5] NAZAROVA T, LISDAT C, RIEHLE F, et al. Low-frequency-noise diode laser for atom interferometry [J]. Journal of the Optical Society of America B, 2008, 25(10): 1632-1638.

[6] MEHMET M, AST S, EBERLE T, et al. Squeezed light at 1550 nm with a quantum noise reduction of 12. 3 dB[J]. Optics Express, 2011, 19(25): 25763-25772.

[7] MORIN O, HUANG K, LIU J, et al. Remote creation of hybrid entanglement between particle-like and wave-like optical qubits[J]. Nature Photonics, 2014, 8(7): 570-574.

[8] JULSGAARD B, KOZHEKIN A, POLZIK E S. Experimental long-lived entanglement of two macroscopic objects [J]. Nature, 2001, 413(6854): 400-403.

[9] WILSON D J, REGAL C A, PAPP S B, et al. Cavity optomechanics with stoichiometric SiN films[J]. Physical Review Letters, 2009, 103(20): 207204.

[10] JAYICH A M, SANKEY J C, BORKJE K, et al. Cryogenic optomechanics with a Si3N4 membrane and classical laser noise[J]. New Journal of Physics, 2012, 14(11): 115018.

[11] PURDY T P, YU P L, PETERSON R W, et al. Strong optomechanical squeezing of light[J]. Physical Review X, 2013, 3(13): 031012.

[12] PHELPS G A, MEYSTRE P. Laser phase noise effects on the dynamics of optomechanical resonators [J]. Physical Review A, 2011, 83(6): 063838.

[13] SAFAVI-NAEINI A H, CHAN J, HILL J T, et al. Laser noise in cavity-optomechanical cooling and thermometry[J]. New Journal of Physics, 2013, 15(3): 035007.

[14] KWEE P, WILLKE B, DANZMANN K. Shot-noise-limited laser power stabilization with a high-power photodiode array [J]. Optics Letter, 2009, 34(19): 2912-2914.

[15] HARB C C, GRAY M B, BACHOR H A, et al. Suppression of the intensity noise in a diode-pumped neodymium: YAG nonplanar ring laser [J]. IEEE Journal of Quantum Electronics, 1994, 30(12): 2907-2913.

[16] WILLKE B, UEHARA N, GUSTAFSON E K, et al. Spatial and temporal filtering of a 10-W Nd:YAG laser with a Fabry-Perot ring-cavity premode cleaner[J]. Optics Letter, 1998, 23(21): 1704-1706.

[17] HALD J, RUSEVA V. Efficient suppression of diode-laser phase noise by optical filtering[J]. Journal of the Optical Society of America B, 2005, 22(11): 2338-2344.

[18] GRAY M B, CHOW J H, MCKENZIE K, et al. Using a passive fiber ring cavity to generate shot-noise-limited laser light for low-power quantum optics applications[J]. IEEE Photonics Technology Letter, 2007, 19(14): 1063-1065.

[19] NGUYEN T T H, CHOW J H, MOW-LOWRY C M, et al. A shot-noise limited fiber laser source by cascaded passive optical filtering[J]. IEEE Journal of Quantum Electronics, 2010, 46(6): 976-980.

[20] INOUE S, YAMAMOTO Y. Longitudinal-mode-partition noise in a semiconductor-laser-based interferometer [J]. Optics Letter, 1997, 22(5): 328-330.

[21] GLÖCKL O, ANDERSEN U L, LORENZ S, et al. Sub-shot-noise phase quadrature measurement of intense light beams[J]. Optics Letter, 2004, 29(16): 1936-1938.

[22] HUNTINGTON E H, MILFORD G N, ROBILLIARD C, et al. Demonstration of the spatial separation of the entangled quantum sidebands of an optical field[J]. Physical Review A, 2005, 71(4): 041802.

[23] SHELBY R M, LEVENSON M D, BAYER P W. Resolved forward Brillouin scattering in optical fibers [J]. Physical Review Letter, 1985, 54(9): 939-942.